

## Chapter 2

# Compact Modeling of High-Speed Interconnects

High-speed interconnects are essentially planar transmission lines. The fundamental mode of propagation in transmission line interconnects is the transverse electromagnetic (TEM) wave [1]. In ideal case, when the conductivity of the line is infinity the basic mode of propagation would be the TEM mode. This is assuming that the medium in which the line is embedded is considered to be homogeneous, lossless and isotropic. However for most practical cases, the lines have finite conductivity that results in a deviation from the TEM mode. The properties of the dielectric material are also far from ideal with dielectric losses dominating conductor losses as frequency scales up. Therefore, interconnect lines embedded in inhomogeneous substrates cannot support pure TEM mode. The modified mode of propagation has small axial components of the electric and magnetic fields. The field distribution in such a non-ideal transmission line interconnect closely represents the ideal TEM mode with negligible electric/magnetic field components and is called the quasi-TEM mode [1, 2]. Transmission line theory has two aspects: In one case, the propagation of electromagnetic waves is studied when the characteristic parameters of the line are given. In the other case, the conductor geometry is known and the line parameters such as the characteristic impedance, attenuation constant, propagation constant and the shunt capacitance are to be obtained. This aspect is particularly suited for interconnect design and analysis. With the quasi-TEM approximation, the calculation of these line parameters requires the solution of the two-dimensional Laplace's equation. This solution is based on the computation of the boundary conditions governed by the geometry of the line.

There are many analytical techniques available in the literature for the solution of the Laplace's equation. This chapter presents a qualitative overview of some of the most commonly used analytical techniques, which includes, among others, the conformal transformation method [1, 3–6], the finite-difference method [7–10] and the variational method [1, 2, 11–13]. In the following section, a comparative overview of these techniques is presented. In the latter half of this chapter, we propose the application of a unified approach for analysis of high-speed

interconnects. Based on the comparative summary of the major analytical approaches and the relative advantages of this unified approach; we feel that this technique is well suited for planar chip–chip interconnects. Derivation of line parameters using a unified approach that combines the variational method with the transverse transmission line technique [2, 14] is presented. This chapter makes an attempt to highlight the relative advantages and applicability of the unified approach and concludes that this technique fits in our analytical models better than other available methods. Although the comparison presented in the next section is qualitative only, it would provide reasonable insight to the reader; further leaving a scope for the employment of above-listed techniques to be used in the modeling of high-speed interconnects.

## 2.1 Review of the Analytical Methods

A lot of research has been presented in the past on transmission line modeling. Most of the earlier works focused on problems in *MICs* and other microwave circuits. However, with the signal frequencies now entering well into the GHz range, it is only appropriate to apply some of these analytical techniques to address signal integrity issues in high-speed VLSI and chip–chip interconnects. The techniques available to solve TEM and quasi-TEM problems can be broadly classified into two classes, namely exact and approximate [15]. Some of the most common approaches under these two classes are shown in Fig. 2.1.

Since most of these techniques are extensively covered in the published research on microwave theory; we will only highlight their relative merits and drawbacks with an objective to justify the choice of the method of analysis used in this book. The formulae obtained using conformal mapping are derived using the Schwartz-Christoffel conformal transformation. This method enables one to evaluate the capacitances and characteristic impedance between straight-sided conductors when the problem can be reduced to two dimensions, for example the cross-section plane of a transmission line. The boundary of the cross-section is transformed into a simpler boundary for which the solution is known using transformations in the complex plane. Finally the capacitance and characteristic impedance of the original boundary are equal to the respective quantities of the transformed boundary [4, 5]. The conformal transformation technique is exact and accurate. Since, the capacitance term of each element retains the correct dependencies on the line geometry; we require very few 2D simulations resulting in lesser computational time. However, in case of transmission lines with inhomogeneous medium the application of conformal transformation may become quite complicated. To overcome this problem, the Discrete Variational Conformal (DVC) transformation method suggested by Diaz [15] seems to be more suitable in cases where the geometry of the structure under analysis is not simple. However, in case of microstrip-like interconnects (that are commonly encountered in chip–chip interconnects) the DVC method provides results that are virtually identical.

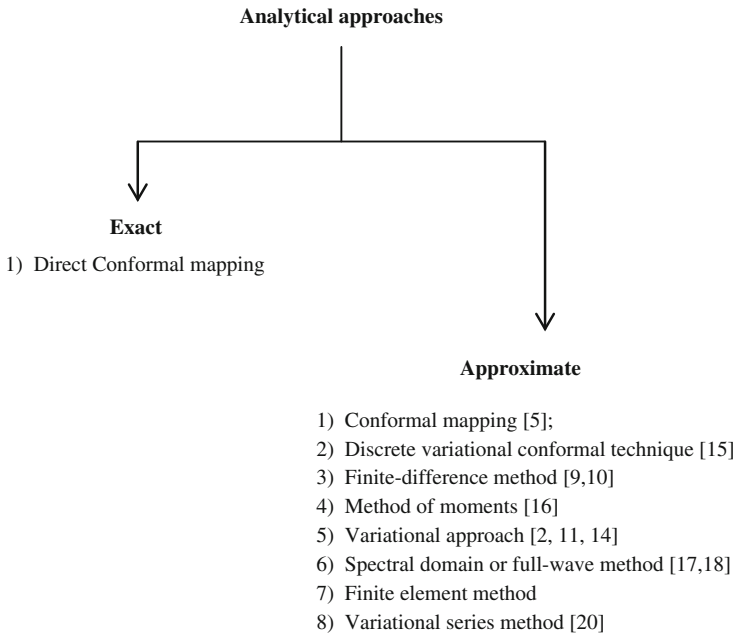


**Fig. 2.1** Classification of analytical methods. © 1986 IEEE reprinted, with permission, from Diaz [15]

Finite-difference method is also widely used for analysis of planar transmission lines. The application of the finite-difference method to TEM transmission lines involves the solution of Laplace's equation in the cross-sectional plane subject to boundary conditions on the inner and the outer conductors. The entire domain between the conductors is divided into a finite set of mesh points. Laplace's equation is then solved in the finite-difference form by digital computation [14]. This method can be applied to TEM lines and has been extended to quasi-TEM transmission lines with limited inhomogeneity and is elaborately explained in [7, 8]. However, the finite-difference technique is vastly limited to homogeneous and geometrically simpler structures. With complex interconnect layout designers do not have the luxury to assume such simplifications. The accuracy of the method depends on the fineness of the mesh size (as in coupled strip transmission lines). This results in very large set of equations to be solved, leading to the problem of convergence and therefore inaccuracy. Kammler's method given in [16] can be used to analyze interconnects with multiple layers of dielectrics, but it may prove to be computationally cumbersome. Other techniques like the finite element method and the spectral domain analysis also suffer from problems in analyzing open microstrip cases and thus have limited applications. In case of open multi-dielectric planar lines, the application of finite elements leads to two difficulties; namely.

- the infinite field extension due to the open structure,
- and, the field singularities caused by the conductor edges.

A combined approach making use of the variational series based on the conformal transformation has been reported by Smith [19]. This method overcomes the difficulties of convergence and singularities encountered in the finite-difference method and/or finite elements.

Finally, the variational method [2, 11, 14] is generally applied to those problems where the physical system under study acts so that some function of its behavior attains the least or the greatest value. The variational method can be used to obtain the expression for line capacitance of a transmission line in an inhomogeneous, isotropic/anisotropic media. This geometrical environment is exactly the case in high-speed interconnects. When combined with the transverse transmission line technique of determining the Green's function [7, 8, 20], line parameters can be computed for a variety of structures. The method is simple and generalized due to the ease of computing Green's function using the transverse transmission line technique and gives fairly accurate results without much computational effort. This method has certain limitations also; namely

- dielectric material should be of low loss,
- the method assumes a TEM mode and neglects radiation effects,
- and, the accuracy of the results depends on the trial function.

In case of the modern day interconnect design the above-mentioned points are largely taken care of. Also, the trial function can be chosen after experimental verification leaving lesser scope for inaccuracy. To summarize the above discussion, the authors feel that the variational analysis in the space domain combined with the transverse transmission line technique offers a robust approach for analysis of high-speed transmission line interconnects. The conformal mapping technique can be very complicated in the case of inhomogeneous interconnects. Modern IC layouts cannot certainly guarantee homogeneity. Also, the finite-difference method involves a numerical evaluation and is thus limited to simpler structures. The other listed techniques have even less applicability than these methods. The variational method—though approximate—offers a simpler way of determining propagation parameters including line parasitics. When combined with the transverse transmission line technique of determining the Green's function [7, 8, 15], the derivation for the capacitance of the interconnect line becomes quite simple and reasonably accurate and is therefore suited for CAD applications. Since the variational method treats the dielectric boundary conditions in a generalized way, it is possible to analyze multilayer interconnect lines. The accuracy of this method is insensitive to the choice of the trial function (discussed in the following sections). Authors in [14] suggest that it is possible to take into account all the dielectric boundary conditions no matter how many planar boundaries exist in these lines. The method is based on the calculation of the line capacitance by the static field theory and therefore is an approximation to EM theory. It is felt that unlike conformal mapping and other mentioned techniques—which are also static

field theories—the analytical treatment of multiple boundaries is easier by the variational method [2, 14]. The computational time is also far less than for other techniques which makes it suitable for CAD-related applications.

The above discussion illustrates the possible application of variational method combined with the transverse transmission line technique for the analysis of the chip–chip interconnects. However, interested readers are strongly encouraged to read the literature presented by authors in [7, 14, 20]. It is felt that the method is explained in detail in these literatures.

## 2.2 Unified Approach

Classically speaking the unified approach refers to the variational analysis combined with the transverse transmission line technique. The approach was first reported for analysis of Microwave Integrated Circuit (MIC), Monolithic Microwave Integrated Circuit (MMIC) and planar transmission lines. In this approach, the expression for the capacitance of a transmission line is determined by the variational technique. The Green's function is computed using the transverse transmission line technique in the space domain. In this section, derivation for the line capacitance using unified approach is reproduced from the historical literatures for both single as well as coupled line structures.

### 2.2.1 Computing Green's Function

Let us assume a unit charge located at  $(x_o, y_o)$  as shown in Fig. 2.2. The Green's function should satisfy the Poisson's differential equation in the  $x$ – $y$  plane and is given by:

$$\nabla_t^2 G(x, y/x_o, y_o) = -\frac{1}{\epsilon} \delta(x - x_o) \cdot \delta(y - y_o) \quad (2.1)$$

For an interconnect line over a multilayered substrate, the boundaries at the interface of the dielectrics are given by:

$$G(x, s_{j-0}) = G(x, s_{j+0}) \quad (2.2)$$

$$\epsilon_j \frac{\partial G(x, s_{j-0})}{\partial y} = \epsilon_{j+1} \frac{\partial G(x, s_{j+0})}{\partial y} \quad (2.3)$$

Figure 2.3a, b represent the configuration corresponding to a microstrip line with rectangular side walls and a corresponding geometry required to compute the Green's function.

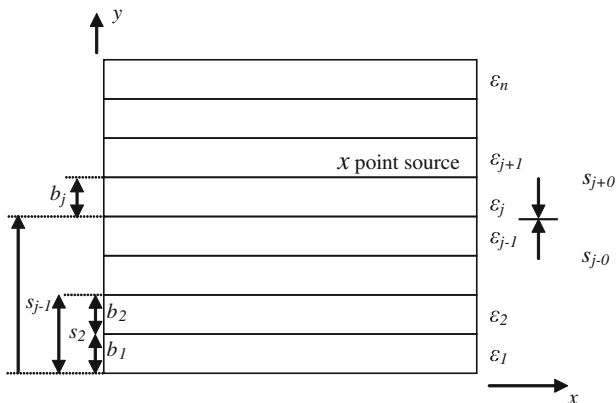


**Fig. 2.2** Geometry of an n-layer dielectric with side walls and a point charge at  $(x_0, y_0)$ . © 1978 IEEE reprinted, with permission, from Crampagne et al. [20]

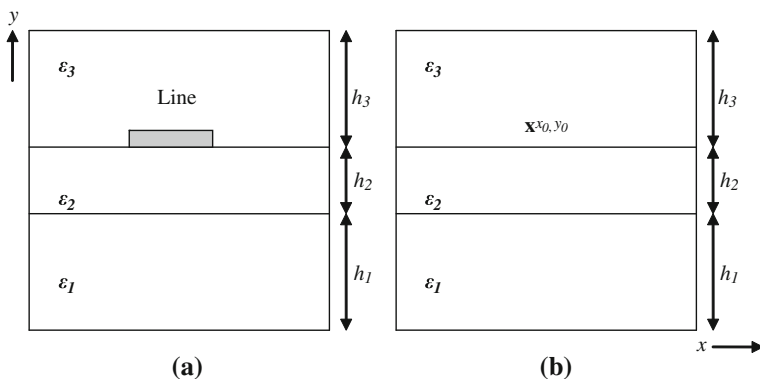


**Fig. 2.3** **a** Microstrip line with rectangular side walls. **b** Geometry to calculate the Green's function. © 1978 IEEE reprinted, with permission, from Crampagne et al. [20]

Figure 2.3 represents only a particular case and the number of cases depends on the boundary conditions at the rectangular walls. The boundary conditions satisfied at the vertical walls can be either of the Dirichlet type (electric wall,  $G = 0$ ) or of the Neumann type (magnetic wall,  $\partial G / \partial n = 0$ ). The boundary conditions on the lower and upper surfaces (or horizontal walls) can be taken into account using the transverse transmission line technique and will be discussed later. If we assume any arbitrary conditions on the horizontal walls, then there could be three specific cases of boundary conditions on the vertical walls as shown in Fig. 2.4.

The Green's function can be expressed as the summation of the product of elementary functions given below:

$$G = \sum_n G_n(x) G_n(y) \quad (2.4)$$

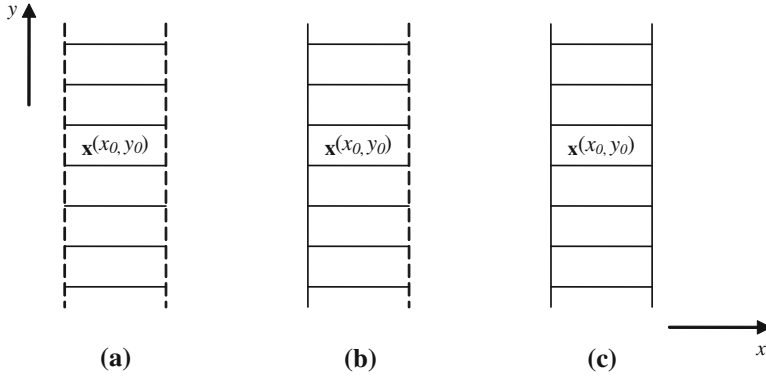


**Fig. 2.4** Magnetic (solid line) and electric (dashed line) boundaries. © 1978 IEEE reprinted, with permission, from Crampagne et al. [20]

We should now derive the identities  $G_n(x)$  and  $G_n(y)$ . In order to satisfy the boundary conditions on the vertical walls separated by wall spacing  $c$ , the following expressions are found for  $G_n(x)$  for three separate cases corresponding to Fig. 2.4.

*Case a* Electric wall at  $x = 0$  and  $c$ :

$$G_n(x) = \sin \frac{n\pi x}{c}, \quad n = 1, 2, \dots, \infty \quad (2.5)$$

*Case b* Electric wall at  $x = 0$  and magnetic wall at  $x = c$ :

$$G_n(x) = \sin \frac{(2n+1)\pi x}{2c}, \quad n = 0, 1, 2, \dots, \infty \quad (2.6)$$

*Case c* Magnetic walls at  $x = 0$  and  $c$ :

$$G_n(x) = \cos \frac{n\pi x}{c}, \quad n = 2, 3, \dots, \infty \quad (2.7)$$

It is seen that the functions,  $\sin(n\pi x/c)$ ,  $\sin[(2n+1)\pi x/2c]$  and  $\cos(n\pi x/c)$  are orthogonal in the interval  $(0, c)$ . Substituting the expressions in (2.5)–(2.7) the following differential equations are obtained:

*Case a*

$$\left[ \frac{d^2}{dy^2} - \left( \frac{n\pi}{c} \right)^2 \right] G_n(y) = -\frac{2}{c\epsilon} \delta(y - y_o) \sin \frac{n\pi x_o}{c} \quad (2.8)$$

*Case b*

$$\left[ \frac{d^2}{dy^2} - \left( \frac{(2n+1)\pi}{2c} \right)^2 \right] G_n(y) = -\frac{2}{c\epsilon} \delta(y - y_o) \sin \frac{(2n+1)\pi x_o}{2c} \quad (2.9)$$

Case c

$$\left[ \frac{d^2}{dy^2} - \left( \frac{n\pi}{c} \right)^2 \right] G_n(y) = -\frac{2}{c\epsilon} \delta(y - y_o) \cos \frac{n\pi x_o}{c} \quad (2.10)$$

The Green's function,  $G$  and  $G_n(y)$ , should satisfy the boundary conditions at the various dielectric interfaces given by Eqs. (2.2) and (2.3).

### 2.2.2 Transverse Transmission Line Technique

Having derived  $G_n(x)$  in the last section we now compute the identity  $G_n(y)$ . The Transverse transmission line technique provides a simpler method that numerically evaluates the Green's function. For  $N$  number of dielectric layers, the solution of above differential equations leads to a set on linear equations with  $2N$  number of rows. Consider a transmission line with a current source of intensity  $I_s$  at the charge plane  $y = y_o$ . The voltage and current relations along the line are found to be:

$$\frac{dV}{dy} = -\gamma Z I_s \quad (2.11)$$

$$\frac{dI}{dy} = -\frac{\gamma}{Z} V + I_s \delta(y - y_o) \quad (2.12)$$

Here,  $Z$  is the characteristic impedance of the line and  $\gamma$  is the propagation constant. Solving (2.11) and (2.12), we get:

$$\frac{d^2 V}{dy^2} - \gamma^2 V = -\gamma Z_c I_s \delta(y - y_o) \quad (2.13)$$

If we consider the transmission line as a set of stepped characteristic admittances in parallel with  $Y_{cj}$  as the characteristic admittance of the  $j$ th section of transmission line, then the continuity conditions at the interfaces between the two differential admittances are given by:

$$V_j = V_{j+1} \quad (2.14)$$

and  $I_{-j} = I_{j+1}$ . Thus we get:

$$Y_{cj} \frac{\partial V_j}{\partial y} = Y_{cj+1} \frac{\partial V_{j+1}}{\partial y} \quad (2.15)$$



Comparing Eqs. (2.13), (2.14) and (2.15), author in [14] came up with the following similarities:

1. The functions characterizing the Green's function can be identified by the voltage along the line.

$$V \equiv G_n(y) \quad (2.16)$$

2. The dielectric constant of the  $j$ th layer can be identified by the characteristic admittance of the transmission line for that section.

$$Y_{cj} = \varepsilon_j \quad (2.17)$$

Thus, the boundary conditions satisfied by the Green's function at the various dielectric interfaces are equivalent to the boundary conditions satisfied by the voltages at the interfaces between two dissimilar characteristic admittances. The voltage on the transmission line at  $y = y_o$  is given by:

$$V|_{y=y_o} = \frac{I_s}{Y} \quad (2.18)$$

where  $Y$  is the admittance at  $y = y_o$ . We can now obtain the Green's function for the three cases listed in Fig. 2.4 as given by [14]:

*Case a*

$$Z = \frac{1}{\varepsilon}, \quad \gamma = \frac{n\pi}{c}, \quad \text{and} \quad I_s = \frac{2}{n\pi} \sin \frac{n\pi x_o}{c}$$

$$G_n(y)|_{y=y_o} = \frac{2}{n\pi Y} \sin \frac{n\pi x_o}{c} \quad (2.19)$$

Substituting (2.5) and (2.19) in (2.4), the Green's function at the charge plane  $y = y_o$  becomes:

$$G(x, y/x_o, y_o)|_{y=y_o} = \sum_{n=1}^{\infty} \frac{2}{n\pi Y} \sin \frac{n\pi x}{c} \sin \frac{n\pi x_o}{c} \quad (2.20)$$

*Case b*

$$Z = \frac{1}{\varepsilon}, \quad \gamma = \frac{(2n+1)\pi}{2c}, \quad \text{and} \quad I_s = \frac{4}{(2n+1)\pi} \sin \frac{(2n+1)\pi x_o}{2c}$$

$$G_n(y)|_{y=y_o} = \frac{4}{(2n+1)\pi Y} \sin \frac{(2n+1)\pi x_o}{2c} \quad (2.21)$$

Substituting (2.6) and (2.21) in (2.4), the Green's function at the charge plane  $y = y_o$  becomes:

$$G(x, y/x_o, y_o)|_{y=y_o} = \sum_{n=0}^{\infty} \frac{4}{(2n+1)\pi Y} \sin \frac{(2n+1)\pi x}{2c} \sin \frac{(2n+1)\pi x_o}{2c} \quad (2.22)$$

Case c

$$Z = \frac{1}{\varepsilon}, \quad \gamma = \frac{n\pi}{c}, \quad \text{and} \quad I_s = \frac{2}{n\pi} \cos \frac{n\pi x_o}{c}$$

$$G_n(y)|_{y=y_o} = \frac{2}{n\pi Y} \cos \frac{n\pi x_o}{c} \quad (2.23)$$

Substituting (2.7) and (2.23) in (2.4), the Green's function at the charge plane  $y = y_o$  becomes:

$$G(x, y/x_o, y_o)|_{y=y_o} = \sum_{n=1}^{\infty} \frac{2}{n\pi Y} \cos \frac{n\pi x}{c} \cos \frac{n\pi x_o}{c} \quad (2.24)$$

We can now see that the Green's function can be deduced from the admittance  $Y$  that can be obtained using the standard transmission line admittance equation. As mentioned earlier the unified approach is a combination of the variational technique and the transverse transmission line technique. In that the Green's function is computed using the latter as shown in the preceding discussion. Table 2.1 gives the identification of all the characteristic parameters concerned in the above discussion.

### 2.2.3 Variational Method

In the unified approach the variational method is used to compute the capacitance per unit length [1]. Let us consider a system of perfect conductors  $S_1, S_2, \dots, S_N$  with  $Q_1, Q_2, \dots, Q_N$  as the charges on the conductors and  $V_1, V_2, \dots, V_N$  as the potential difference. The potential function  $\varphi$  in the space domain happens to be the solution of the Laplace's equation. The electrostatic energy stored in such a system would be given by:

$$W_e = \frac{\varepsilon}{2} \int_{vol} \nabla \varphi \cdot \nabla \varphi dV \quad (2.25)$$

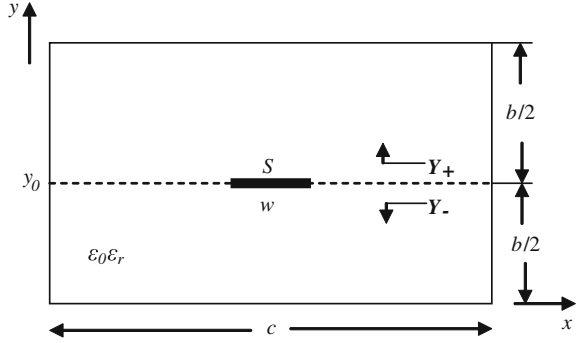
There could be an incremental change in the energy function due to displacement of charges from their mean position. This is given by:

$$\delta W_e = \frac{\varepsilon}{2} \left[ \int_{vol} \nabla \delta \varphi \cdot \nabla \delta \varphi dV \right] \quad (2.26)$$

**Table 2.1** Various identities based on boundary conditions (courtesy of Crampagne et al. [20])

Geometric configuration	Formula to obtain Green's function	Differential equation	$\gamma$	$I_s$
Electric wall at $x = 0$ and $c$	$G = \sum_{n=1}^{\infty} G_n(y) \sin \frac{n\pi x}{c}$	$\left[ \frac{d^2}{dy^2} - \left( \frac{n\pi}{c} \right)^2 \right] G_n(y) = -\frac{2}{c^2} \delta(y - y_o) \sin \frac{n\pi x_o}{c}$	$\frac{n\pi}{c}$	$\frac{2}{n\pi} \sin \frac{n\pi x_o}{c}$
Electric wall at $x = 0$ and magnetic wall at $x = c$	$G = \sum_{n=0}^{\infty} G_n(y) \sin \frac{(2n+1)\pi x}{2c}$	$\left[ \frac{d^2}{dy^2} - \left( \frac{(2n+1)\pi}{2c} \right)^2 \right] G_n(y) = -\frac{2}{c^2} \delta(y - y_o) \sin \frac{(2n+1)\pi x_o}{2c}$	$\frac{(2n+1)\pi}{2c}$	$\frac{4}{(2n+1)\pi} \sin \frac{(2n+1)\pi x_o}{2c}$
Magnetic walls at $x = 0$ and $c$	$G = \sum_{n=1}^{\infty} G_n(y) \cos \frac{n\pi x}{c}$	$\left[ \frac{d^2}{dy^2} - \left( \frac{n\pi}{c} \right)^2 \right] G_n(y) = -\frac{2}{c^2} \delta(y - y_o) \cos \frac{n\pi x_o}{c}$	$\frac{n\pi}{c}$	$\frac{2}{n\pi} \cos \frac{n\pi x_o}{c}$

**Fig. 2.5** Lateral view of general microstrip-like interconnect structure.  
© 1982 IEEE reprinted, with permission, from Bhat and Koul [2]



Authors in [1, 14] have elaborated on the upper and lower bounds of this capacitance. The upper bound on capacitance per unit length of the line is given by:

$$C = \frac{\varepsilon}{V_o^2} \iint_{xy\text{-plane}} |\nabla_t \phi|^2 dx dy = \frac{\varepsilon \iint_{xy\text{-plane}} |\nabla_t \phi|^2 dx dy}{\left( \int_{S_1}^{S_2} \nabla_t \phi \cdot dl \right)^2} \quad (2.27)$$

where,  $V_o$  is the line integral of  $\nabla_t \phi$  from  $S_1$  to  $S_2$ . For an approximate value of  $\phi$ , the calculated value of  $C$  will always be greater than the true value.

Similarly, the lower bound on capacitance is given by:

$$\frac{1}{C} = \frac{1}{Q^2} \int_{S_2} \phi(x, y) \rho(x, y) dl \quad (2.28)$$

Note that for any trial function  $\rho(x_o, y_o)$ , the calculated value of  $1/C$  is always larger than the true value, which defines the lower bound. We now combine the two techniques to compute the capacitance per unit length for single and coupled transmission line interconnects.

### 2.2.4 Unified Approach for Calculation of Capacitance Per Unit Length for Single Interconnect Lines

In the earlier section we have derived the variational expression for the capacitance of any two-conductor line having an arbitrary cross-section, as shown in Fig. 2.5. For such an interconnect geometry the charge distribution is given as:

$$\rho(x, y) = f(x) \delta(y - y_o) \quad (2.29)$$

Substituting this charge distribution function in (2.28), the variational formula for the capacitance per unit length for a multilayer structure with side walls is given as:

$$\frac{1}{C} = \frac{\int_S \int_S G(x, y/x_o, y_o) f(x) dx dx_o}{\left[ \int_S f(x) dx \right]^2} \quad (2.30)$$

Here, Green's function for various boundary conditions derived in the previous section as (2.20), (2.22) and (2.24) can be substituted in (2.29). We get the expressions for capacitance for the three cases of boundary conditions as:

*Case a*

$$C = \frac{\left[ \int_S f(x) dx \right]^2}{\sum_{n=1}^{\infty} \frac{2}{n\pi Y} \left[ \int_S f(x) \sin \frac{n\pi x}{c} dx \right]^2} \quad (2.31)$$

*Case b*

$$C = \frac{\left[ \int_S f(x) dx \right]^2}{\sum_{n=0}^{\infty} \frac{4}{(2n+1)\pi Y} \left[ \int_S f(x) \sin \frac{(2n+1)\pi x}{2c} dx \right]^2} \quad (2.32)$$

*Case c*

$$C = \frac{\left[ \int_S f(x) dx \right]^2}{\sum_{n=1}^{\infty} \frac{2}{n\pi Y} \left[ \int_S f(x) \cos \frac{n\pi x}{c} dx \right]^2} \quad (2.33)$$

At any interface of the dielectrics the admittance can be decomposed into two parts: the  $Y_+$  and  $Y_-$  representing the admittances above and below the charge plane, respectively. The total admittance at the charge plane is a parallel combination of these two terms and is therefore a summation of the upper and lower admittances as  $Y = Y_+ + Y_-$ . Using the expression for the input admittance  $Y_{in}$  the admittance of a particular section  $l_j$  can be computed. The input admittance  $Y_{in,j}$  is given by:

$$Y_{in,j} = Y_{cj} \left[ \frac{Y_{lj} + Y_{cj} \tanh(\gamma_j l_j)}{Y_{cj} + Y_{lj} \tanh(\gamma_j l_j)} \right] \quad (2.34)$$

where  $Y_{lj}$  is the load admittance of the  $j$ th section which will be the input admittance  $Y_{in\ j+1}$  of the next  $(j + 1)$ th section. Also,  $Y_{cj}$  and  $\gamma_j$  are the characteristic admittance and propagation constant of the  $j$ th section.

$$Y_{cj} = \varepsilon_j \quad (2.35)$$

and

$$\begin{aligned} \gamma_j &= \gamma = n\pi/c, & \text{for cases (a) and (c)} \\ &= (2n + 1)\pi/2c, & \text{for case (b)} \end{aligned}$$

We now need to calculate the charge distribution  $f(x)$  before performing the integration in capacitance formula above. The charge density is concentrated at the edges of the strip. For such a case, the function is given by:

$$\begin{aligned} f(x) &= \left[ 1 - \{(2/w)|x - c/2|\}^2 \right]^{-1} & (c - w)/2 \leq x \leq (c + w)/2 \\ &= 0 & \text{otherwise} \end{aligned} \quad (2.36)$$

Here  $w$  is the width of the strip conductor. Authors in [14] report an accurate trial function and is given by (2.37):

$$\begin{aligned} f(x) &= (1/w)[1 + A|(2/w)(x - c/2)|^3], & (c - w)/2 \leq x \leq (c + w)/2 \\ &= 0 & \text{otherwise} \end{aligned} \quad (2.37)$$

Substituting (2.37) in (2.31) and simplifying, the unified formula for capacitance per unit length is:

$$C = \frac{(1 + 0.25A)^2}{\sum_{n \text{ odd}} \left( (L_n + AM_n)^2 P_n / Y \right)} \quad (2.38)$$

where

$$L_n = \sin(\beta_n w/2)$$

$$M_n = (2/\beta_n w)^3 \left[ 3 \left\{ (\beta_n w/2)^2 - 2 \right\} \cos(\beta_n w/2) + (\beta_n w/2) \left\{ (\beta_n w/2)^2 - 6 \right\} \sin(\beta_n w/2) + 6 \right]$$

$$P_n = (2/n\pi)(2/\beta_n w)^2$$

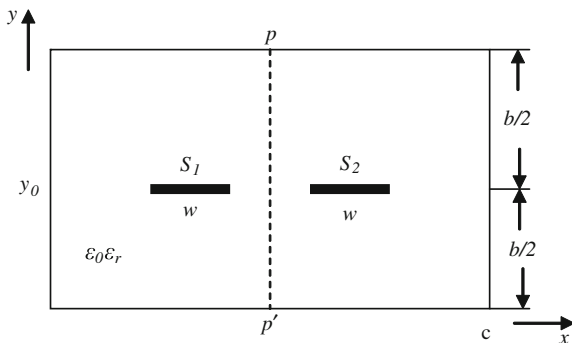
$$\beta_n = n\pi/c$$

$$A = - \frac{\sum_{n \text{ odd}} (L_n - 4M_n) L_n P_n / Y}{\sum_{n \text{ odd}} (L_n - 4M_n) M_n P_n / Y}$$

$$(2.39)$$

Note that in (2.38), we only need to evaluate the admittance  $Y$  at the charge plane depending on the structure under investigation and the corresponding boundaries present.

**Fig. 2.6** Lateral view of edge-coupled microstrip-like interconnect structure.  
© 1982 IEEE reprinted, with permission, from Bhat and Koul. [2]



### 2.2.5 Unified Approach for Calculation of Capacitance for Coupled Interconnect Lines

In case of edge-coupled stripline structure, as shown in Fig. 2.6, the even- and odd-mode capacitances can be obtained by placing a magnetic wall and an electric wall, respectively, at the center of the coupled lines, and by considering half the structure between  $x = 0$  and  $x = c/2$ . The even- and odd-mode charge distribution functions are assumed to be of the form given by:

$$f(x)_{\left(\begin{smallmatrix} \text{even} \\ \text{odd} \end{smallmatrix}\right)} = \left(\frac{1}{w}\right) \left[ 1 + A_{\left(\begin{smallmatrix} \text{even} \\ \text{odd} \end{smallmatrix}\right)} \left| \left(\frac{2}{w}\right) (x - (c - s - w)/2) \right|^3 \right], \quad \text{for } ((c - s)/2 - w \leq x \leq (c - s)/2) \\ = 0, \quad \text{otherwise.} \quad (2.40)$$

Applying the transverse transmission line method, the even- and odd-mode Green's function can be expressed as:

$$G(x, y_0/x_0, y_0)_{\left(\begin{smallmatrix} \text{even} \\ \text{odd} \end{smallmatrix}\right)} = \sum_{n\left(\begin{smallmatrix} \text{even} \\ \text{odd} \end{smallmatrix}\right)} (4/n\pi Y) \sin(\beta_n x) \sin(\beta_n x_0), \quad (2.41)$$

where

$$\beta_n = n\pi/c. \quad (2.42)$$

The expression for the admittance  $Y$  at the charge plane  $y = y_0$  for each coupled line structure is the same as that for the corresponding single line conductor configuration (as discussed in the previous subsection). The variational expression for the capacitance  $C$  is given by:

$$C_{\left(\begin{smallmatrix} \text{even} \\ \text{odd} \end{smallmatrix}\right)} = \frac{\left(1 + 0.25A_{\left(\begin{smallmatrix} \text{even} \\ \text{odd} \end{smallmatrix}\right)}\right)^2}{\sum_{n\left(\begin{smallmatrix} \text{odd} \\ \text{even} \end{smallmatrix}\right)} \left( \left( L_n + M_n A_{\left(\begin{smallmatrix} \text{even} \\ \text{odd} \end{smallmatrix}\right)} \right)^2 P_n / Y \right)}, \quad (2.43)$$

where

$$\begin{aligned}
 L_n &= \sin(\beta_n w/2) \sin\left\{\beta_n \left(\frac{c-s-w}{2}\right)\right\}, \\
 M_n &= (2/\beta_n w)^3 \sin\left\{\beta_n \left(\frac{c-s-w}{2}\right)\right\} \left[ 3\left\{(\beta_n w/2)^2 - 2\right\} \cos(\beta_n w/2) \right. \\
 &\quad \left. + (\beta_n w/2) \left\{(\beta_n w/2)^2 - 6\right\} \sin(\beta_n w/2) + 6 \right], \\
 P_n &= (4/n\pi)(2/\beta_n w)^2, \text{ and} \\
 A_{\text{odd}}^{\text{even}} &= -\frac{\sum_{n_{\text{even}}}^{\text{odd}} (L_n - 4M_n) L_n P_n / Y}{\sum_{n_{\text{even}}}^{\text{odd}} (L_n - 4M_n) M_n P_n / Y}.
 \end{aligned} \tag{2.44}$$

### 2.3 Concluding Remarks

This chapter presents detailed derivation of the unified approach. We present a qualitative comparison of some of the widely used analytical techniques for analysis of transmission line interconnects. In that we feel that the unified approach is best suited for parameter extraction, computation of propagation constants and CAD programs. It is simple yet accurate with less computational resources. Chip-chip interconnects are essentially planar transmission lines and this technique can be used for analysis of single edge- and broadside-coupled interconnects.

The unified approach essentially combines transverse transmission line technique for computation of Green's function with the variational method for capacitance calculations. Nowadays, high-speed interconnects have a complex layout with presence or absence of ground. This technique can be very efficiently used to address these modified boundary conditions. In the next chapter we shall illustrate the application of this technique to such interconnect structures. In that single and coupled interconnects with modified geometrical configurations will be analyzed. These modified geometries suggest recalculation of the admittance parameters based on the appropriate boundary conditions. The authors strongly recommend further reading of the unified approach and other techniques proposed by authors in [1, 2, 7, 20] for greater understanding of analytical approaches that can be used in developing compact interconnect models.

### References

1. R.E. Collin, *Field Theory of Guided Waves* (McGraw-Hill, New York, 1960)
2. B. Bhat, S.K. Koul, Unified approach to solve a class of strip and microstrip-like transmission lines. *IEEE Trans. Microw. Theory Tech.* **82**(5), 679–686 (1982)



3. L.A. Pipes, *Applied Mathematics for Engineers and Physicists* (McGraw-Hill, New York, 1958)
4. S.B. Cohn, Shielded coupled-strip transmission line. *IRE Trans. Microw. Theory Tech.* **3**(5), 29–38 (1955)
5. S.B. Cohn, Characteristic impedances of broadside-coupled strip transmission lines. *IRE Trans. Microw. Theory Tech.* **8**(6), 633–637 (1960)
6. J.P. Shelton, Impedances of offset parallel-coupled strip transmission lines. *IEEE Trans. Microw. Theory Tech.* **14**(1), 7–14 (1966)
7. H.E. Green, The numerical solution of some important transmission line problems. *IEEE Trans. Microw. Theory Tech.* **13**(5), 676–692 (1965)
8. M.V. Schneider, Computation of impedance and attenuation of tem lines by finite-difference methods. *IEEE Trans. Microw. Theory Tech.* **13**(6), 793–800 (1965)
9. J.G. Yook, N.I. Dib, L.P.B. Raheti, Characterization of high frequency interconnects using finite difference time domain and finite element method. *IEEE Trans. Microw. Theory Tech.* **42**(9), 1727–1736 (1994)
10. O.S. Rosales, D. Suster, Finite-difference computation of the characteristic impedance of unbounded striplines and microstrip lines, in *Proceedings of the 1st IEEE International Caracas Conference on Devices, Circuits and Systems*, (1995) p. 323–327
11. B.N. Das, K.V.S.V.R. Prasad, A generalized formulation of electromagnetically-coupled striplines. *IEEE Trans. Microw. Theory Tech.* **32**(11), 1427–1433 (1984)
12. E. Yamashita, Variational method for the analysis of microstrip-like transmission lines. *IEEE Trans. Microw. Theory Tech.* **16**(8), 529–535 (1968)
13. E. Yamashita, R. Mitra, Variational method for the analysis of microstrip lines. *IEEE Trans. Microw. Theory Tech.* **16**(4), 251–256 (1968)
14. B. Bhat, S.K. Koul, *Stripline-like Transmission Lines for Microwave Integrated Circuits* (Wiley, New York, 1989)
15. R.E. Diaz, The discrete variational conformal technique for the calculation of strip transmission line parameters. *IEEE Trans. Microw. Theory Tech.* **34**(6), 714–722 (1986)
16. D.W. Kammler, Calculation of characteristic admittances and coupling coefficients for strip transmission lines. *IEEE Trans. Microw. Theory Tech.* **16**(11), 925–937 (1968)
17. T. Itoh, R. Mittra, A technique for computing dispersion characteristics of shielded microstrip lines. *IEEE Trans. Microw. Theory Tech.* **22**(10), 896–898 (1974)
18. J.B. Davies, D. Mirshekar-Syahkaf, Spectral domain solution of arbitrary transmission line with multilayer substrate. *IEEE Trans. Microw. Theory Tech.* **25**(2), 143–146 (1977)
19. J.I. Smith, The even- and odd-mode capacitance parameters for coupled lines in suspended substrate. *IEEE Trans. Microw. Theory Tech.* **19**(5), 424–431 (1971)
20. R. Crampagne, M. Ahmadpanah, J.L. Guiraud, A simple method for determining the green's function for a large class of MIC lines having multilayered dielectric substrates. *IEEE Trans. Microw. Theory Tech.* **26**(2), 82–87 (1978)

Compact Models and Measurement Techniques for  
High-Speed Interconnects

Sharma, R.; Chakravarty, T.

2012, XVIII, 69 p. 29 illus., 6 illus. in color., Softcover

ISBN: 978-1-4614-1070-6